

## Enhanced efficiency of organic light-emitting devices with corrugated nanostructures based on soft nano-imprinting lithography

Yue-Feng Liu, Ming-Hui An, Xu-Lin Zhang, Yan-Gang Bi, Da Yin, Yi-Fan Zhang, Jing Feng, and Hong-Bo Sun

Citation: [Applied Physics Letters](#) **109**, 193301 (2016); doi: 10.1063/1.4967504

View online: <http://dx.doi.org/10.1063/1.4967504>

View Table of Contents: <http://scitation.aip.org/content/aip/journal/apl/109/19?ver=pdfcov>

Published by the [AIP Publishing](#)

---

### Articles you may be interested in

[Efficient and reliable green organic light-emitting diodes with Cl<sub>2</sub> plasma-etched indium tin oxide anode](#)  
J. Appl. Phys. **112**, 013103 (2012); 10.1063/1.4731713

[Enhanced hole injection in organic light-emitting devices by using Fe<sub>3</sub>O<sub>4</sub> as an anodic buffer layer](#)  
Appl. Phys. Lett. **94**, 223306 (2009); 10.1063/1.3148657

[Organic light-emitting diodes with photonic crystals on glass substrate fabricated by nanoimprint lithography](#)  
Appl. Phys. Lett. **90**, 111114 (2007); 10.1063/1.2713237

[Color-tunable electroluminescence from white organic light-emitting devices through coupled surface plasmons](#)  
Appl. Phys. Lett. **90**, 081106 (2007); 10.1063/1.2645149

[White organic light-emitting diode comprising of blue fluorescence and red phosphorescence](#)  
Appl. Phys. Lett. **86**, 113507 (2005); 10.1063/1.1879108

---

A promotional banner for Applied Physics Reviews. The background is a dark blue gradient with a bright light source on the right, creating a lens flare effect. On the left, there is a small image of the journal cover for Applied Physics Reviews, which features a diagram of a device structure. The main text 'NEW Special Topic Sections' is in large, white, bold letters. Below this, the text 'NOW ONLINE' is in yellow, followed by 'Lithium Niobate Properties and Applications: Reviews of Emerging Trends' in white. The AIP Applied Physics Reviews logo is in the bottom right corner.

**NEW Special Topic Sections**

**NOW ONLINE**  
Lithium Niobate Properties and Applications:  
Reviews of Emerging Trends

**AIP** Applied Physics  
Reviews

## Enhanced efficiency of organic light-emitting devices with corrugated nanostructures based on soft nano-imprinting lithography

Yue-Feng Liu, Ming-Hui An, Xu-Lin Zhang, Yan-Gang Bi, Da Yin, Yi-Fan Zhang, Jing Feng,<sup>a)</sup> and Hong-Bo Sun

State Key Laboratory on Integrated Optoelectronics, College of Electronic Science and Engineering, Jilin University, 2699 Qianjin Street, Changchun 130012, People's Republic of China

(Received 27 June 2016; accepted 30 October 2016; published online 8 November 2016)

An enhanced efficiency organic light-emitting device (OLED) with corrugated nanostructures on a small-molecule organic film has been demonstrated. By patterning the hole transport layer via soft nano-imprinting lithography and coating with Ag, a nanostructured cathode is introduced to enhance the light extraction of the OLED without affecting the flatness and conductivity of the indium-tin-oxide film. Both luminance and current efficiency are improved compared with those of conventional planar devices. The observable improvement in luminance and current efficiency can be ascribed to the surface plasmonic and scattering effects caused by the Ag nanostructures. Moreover, theoretical simulations also demonstrate that the power loss to surface plasmon-polariton modes has been recovered. *Published by AIP Publishing.*  
[\[http://dx.doi.org/10.1063/1.4967504\]](http://dx.doi.org/10.1063/1.4967504)

Organic light-emitting devices (OLEDs) have shown tremendous potential in display and solid-state lighting applications because of their low power consumption, excellent color range, wide viewing angle, high contrast, fast response time, and flexibility.<sup>1–4</sup> However, the light extraction efficiency of a conventional OLED is still limited to as low as 20% and is one of the most important issues for practical device applications. In conventional OLEDs, the majority of the light generated in the organic layers is confined in the form of waveguide (WG) modes<sup>2–9</sup> in organic and indium-tin-oxide (ITO) anode layers (ITO/organic mode) and in surface plasmon-polariton (SPP) mode<sup>10–13</sup> associated with the metallic cathode/organic interface; light is also trapped in the substrate because of the total internal reflection at the glass/air interface (substrate mode).<sup>3,5,6</sup> Introducing a nanostructure with wavelength to subwavelength scale periodicity has been demonstrated to be an effective method to improve the light extraction. The substrate mode can be extracted by introducing a surface modification on the back side of the glass substrate; for example, attaching a commercial microlens array or a light extraction film.<sup>3,5,6</sup> The WG<sup>2,6–9</sup> and SPP<sup>10–13</sup> power losses also can be coupled out by manipulating the propagation of photons in OLEDs and providing an additional momentum to couple the SPP modes into light. However, the extraction of the power loss to WG and SPP modes is more challenging to achieve without deteriorating the device performance because a modification of the internal structure inside the device is required. Several direct patterning methods, such as vacuum deposition through a shadow mask, laser fabrication, photolithography, and inkjet printing, have been widely used. However, all of them suffer from the limitation that nanostructuring has to start from the substrate to avoid the degradation of the OLEDs. The substrate pattern

transmission approach is met with problems such as electronic degradation because the ITO anode has to be sputtered on the corrugated substrates, which increases its surface roughness. It is obvious that the problem may be solved if nanostructures are incorporated in a certain organic functional layer without affecting the flatness of the ITO film.<sup>13–15</sup> Fortunately, soft nano-imprinting lithography is creating opportunities for forming nanostructures on organic materials without any degradation of their electrical and optical properties.<sup>14–17</sup> Moreover, soft nano-imprinting lithography is less costly, has no optical diffraction limit, does not expose the sample to high-energy radiation, and can easily be applied to non-planar surfaces.<sup>9,16–21</sup> In a previous work, You *et al.* have reported patterning the nanostructures on the active layer in polymer solar cells to enhance the power conversion efficiency.<sup>16</sup>

In this study, we have demonstrated an enhanced efficiency OLED with corrugated nanostructures on a small-molecule organic film. By patterning the hole transport layer via soft nano-imprinting lithography and coating with Ag, a nanostructured electrode is introduced to enhance the extraction of the OLED without affecting the flatness and conductivity of the ITO film. From the experimental results, 24% and 20% enhancement in the luminance and current efficiency, respectively, were obtained compared with those of conventional planar devices. The observable improvement in luminance and current efficiency can be ascribed to the weak surface plasmonic and scattering effects caused by the Ag nanostructures. Similar enhancements of luminance and current efficiency also suggest that enhanced efficiency arises from improving the light extraction rather than electrical properties. Moreover, theoretical simulations demonstrate that the power loss to SPP modes has been recovered.

The fabrication process for OLEDs with nanostructures on a hole transport layer is shown in Fig. 1. The photoresist (NOA63, Norland) nanostructures were fabricated by two-beam interference with a 266-nm deep-ultraviolet laser,

<sup>a)</sup> Author to whom correspondence should be addressed. Electronic mail: [jingfeng@jlu.edu.cn](mailto:jingfeng@jlu.edu.cn)

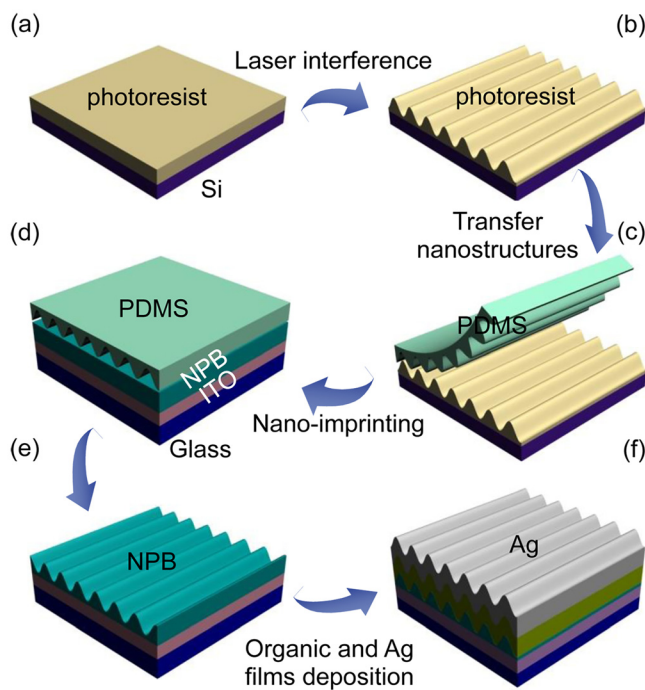


FIG. 1. Schematic fabrication process of a corrugated OLED. (a) Spin coating photoresist, (b) introducing periodic nanostructures by two-beam laser interference lithography, (c) transferring the nanostructures to PDMS, (d) imprinting the nanostructures on NPB hole transparent layer, (e) lifting off the PDMS to obtain NPB nanostructures, and (f) depositing organic and cathode layers.

which has been reported in our previous work.<sup>10–12</sup> These prepared nanostructures were used as master molds. Poly (dimethylsiloxane) (PDMS) was used as an elastomeric imprint mold because it allows for conformal contact with the substrate and easy release because of its high elasticity and flexibility and low surface energy. Silicone elastomer base and curing agent (Dow Corning Co.) with a ratio of 10:1 were well mixed, degassed by a centrifugal process for 5 min at 6000 rpm, dropped onto the prepared master molds, and then baked at 95 °C for 1 h for solidification. Finally, the solidified PDMS film was peeled off from the master and the PDMS mold with the corresponding relief of the master was obtained. Then, the PDMS mold was placed into contact with ITO glass with pre-evaporated metal oxide and organic materials. The stacked structure is ITO/MoO<sub>3</sub> (3 nm)/N,N'-diphenyl-N,N'-bis(1-naphthyl)-(1,1'-biphenyl)-4,4'-diamine (NPB, 70 nm). Then, the whole sample was placed into a vacuum chamber at 10<sup>-2</sup> Pa for 30 min at room temperature. Low vacuum condition can ensure better contact between the PDMS mold and NPB layer. After removal of the PDMS mold, the nanostructures on the surface of NPB layer were obtained. Finally, the emitting layer and cathode were thermally evaporated onto the NPB layer with nanostructures at a rate of 1 Å/s at a base pressure of 5 × 10<sup>-4</sup> Pa. The whole stacked structure of OLED is ITO/MoO<sub>3</sub> (3 nm)/NPB (70 nm)/tris-(8-hydroxyquinoline) aluminum (Alq<sub>3</sub>, 50 nm)/LiF (1 nm)/Al (1 nm)/Ag (80 nm).

In a typical planar OLED structure, the SPP mode is nonradiative because the momenta of SPPs and photons are not matched. Fortunately, momentum compensation can be achieved by applying the corrugated structure at the

nanoscale periodically, making it possible for the SPP mode to reradiate out the energy captured from oscillating dipoles. By taking into account the fact that the SPP resonance at the corrugated metal surface can be tuned by adjusting the nanostructure period, the SPP resonance at the emission wavelength of 532 nm can be obtained by well-designed nanostructures with favorable periods. Theoretical simulation by the finite-difference time-domain (FDTD) method of the absorption peak in the normal direction was performed for the OLEDs with nanostructure periods ranging from 200 to 300 nm to determine the preferred nanostructure period. As shown in Fig. 2(a), the absorption peak for the 250-nm nanostructured device is at approximately 530 nm, which coincides with the emission peak of the emitter (Alq<sub>3</sub>) employed in our devices. As a result, we chose the period of 250 nm for nanostructures introduced into OLEDs. Atomic force microscopy (AFM) images of the nanostructures on the surfaces of NOA63, PDMS, and NPB are shown in Figs. 2(b)–2(d), respectively. It can be clearly seen that the nanostructures have been formed on the surface of the PDMS and NPB layers after transfer and the imprinting process. It should be noted that the height of the transferred and imprinted nanostructures decreased gradually. The heights of NOA63, PDMS, and NPB nanostructures were 74.5 nm, 62.8 nm, and 25.3 nm, respectively. Compared with the PDMS mold, the NPB nanostructures maintained periodicity but were slightly rougher. Combining the properties of the evaporated organic functional layer and the metal film will duplicate the morphology of the NPB layer to form rough metal nanostructures to enhance light extraction by excitation of surface plasmons and scattering.

To illustrate the effects of the imprinted nanostructures on the light extraction of OLEDs, the electroluminescent (EL) performances of the planar and nanostructured OLEDs

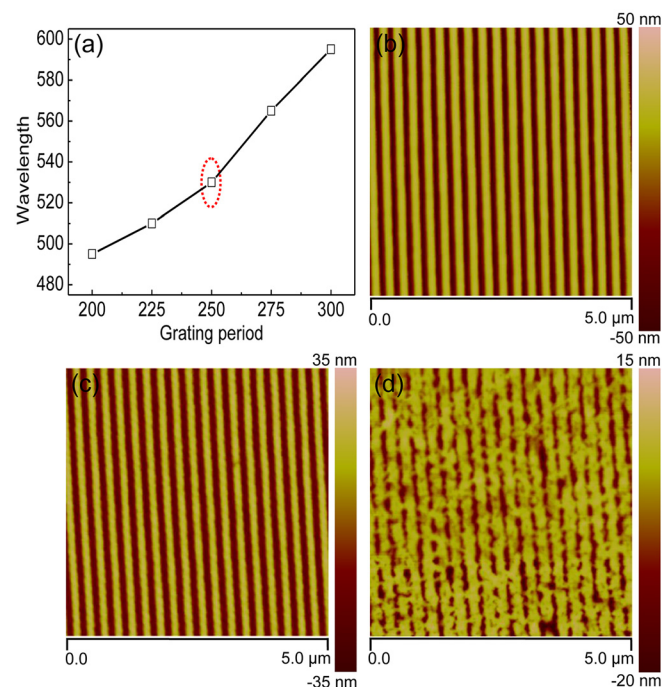


FIG. 2. (a) Simulated SPP resonant wavelength with various periods of nanostructures. AFM images of nanostructures, (b) photoresist, (c) PDMS, and (d) NPB.

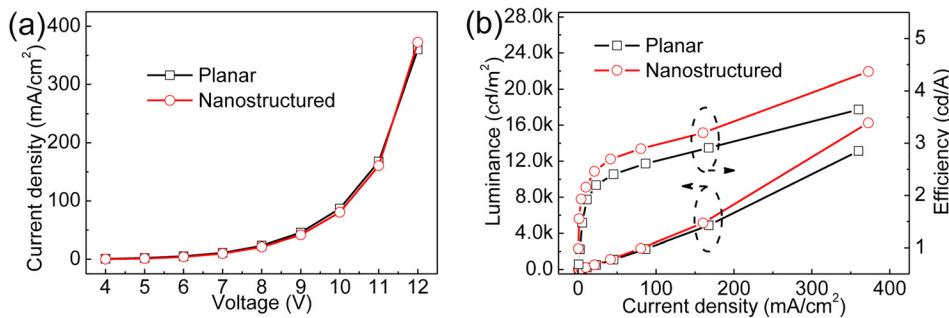


FIG. 3. (a) Current density-voltage and (b) luminance-current density-efficiency characteristics of planar and corrugated OLEDs.

were investigated. Considering that the average thickness of the nanostructured NPB layer decreased from 70 to 50 nm after imprinting, the thickness of the NPB for the planar devices was designed to be 50 nm, so that the effect of the NPB thickness on the hole transport could be excluded. As shown in Fig. 3, the two kinds of devices exhibit almost identical current density-voltage ( $J$ - $V$ ) curves. The nanostructured OLEDs show obvious enhancement in both luminance and efficiency as expected; 24% and 20% enhancements, respectively, compared with planar devices are obtained. These enhancements obviously originate from the improved light extraction induced by the nanostructures. In the case of planar OLEDs, much light is confined in the SPP mode by near field coupling. OLEDs with nanostructures extracted much more light, not only by the excitation and radiation of the SPP modes but also by scattering effects at the cathode/organic interface. Moreover, the coupling strength is related to the height of the nanostructures. We can further enhance the light extraction by optimizing the imprinting process to obtain an optimal height for the nanostructures.

Understanding the enhancement mechanism begins with analyzing the devices by measuring their emission spectra as a function of observation angle. EL spectra with

transverse-magnetic (TM) and transverse-electric (TE) polarizations are shown in Figs. 4(a) and 4(b) for the OLEDs with 250-nm nanostructures. The optical modes appear as additional emission peaks, which shift in wavelength as the angle varies, and are observed in EL spectra with TM polarization, while there are none with TE polarization. It is well-known that SPPs are guided TM polarized electromagnetic surface modes that occur at the interface between a metal and a dielectric. The additional emission peaks in the EL spectra for TM polarization show that the energy of the SPP mode may have been coupled out of the OLEDs to the far field. To clarify the optical modes supported by the nanostructured OLEDs, the dispersion relations and distribution of the magnetic field intensity were simulated by employing a FDTD method, where the FDTD codes were generated in-house. Given an incoming wave from the ITO glass side, the reflection waves were computed. Absorption spectra were obtained from the complementary relationship between reflection and absorption. The dispersion map was derived from the simulated absorption spectra for the corrugated device with 250-nm nanostructures and for TM polarization is shown in Fig. 4(c). The dispersion relation curve constructed from the experimental EL emission spectra with TM polarization is also

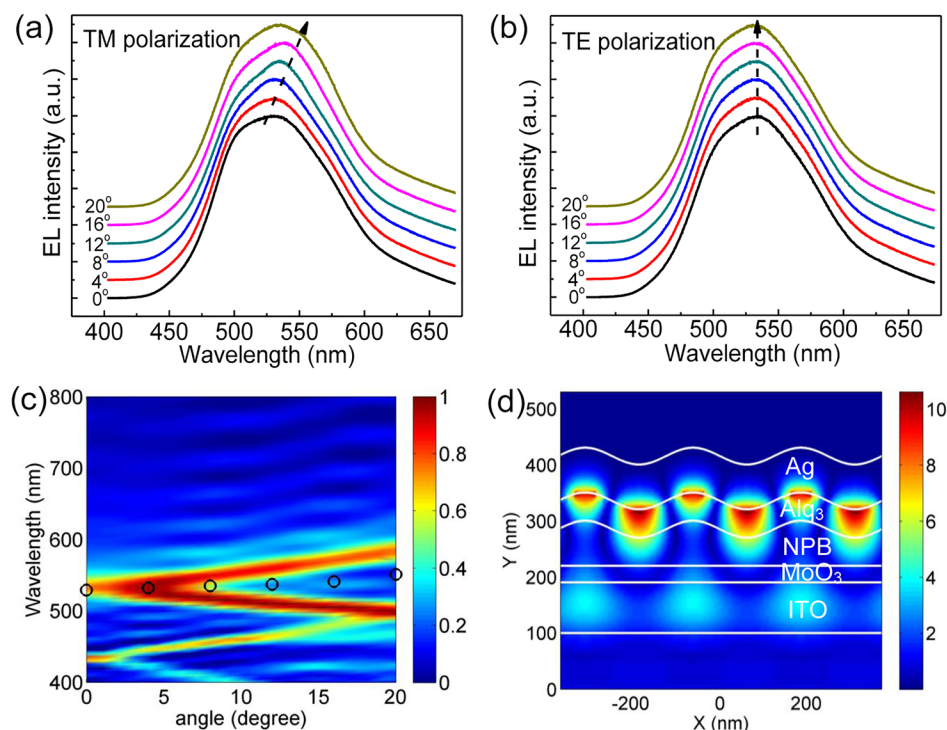


FIG. 4. EL spectra with TM (a) and TE (b) polarization at various observation angles for corrugated OLEDs with 250-nm nanostructures. (c) Calculated and measured (black circles) dispersion relations for TM polarization and (d) calculated distribution of the magnetic field intensity in the corrugated OLEDs at the wavelength of incident polarized light of 532 nm.

plotted in Fig. 4(c). There is agreement between the theoretically calculated absorption spectra and the EL spectra from experimental measurements. This result indicates an efficient outcoupling of light from these optical modes by the appropriate wavelength-scale nanostructure. The spatial magnetic field distribution across the device structure as a function of position with normal incident light was calculated to identify the optical modes for the devices with 250-nm nanostructures. Fig. 4(d) shows the field distribution at the illumination wavelength of 532 nm, which corresponds to the peak wavelength of the EL emission in the normal direction. The field intensity is a maximum at the Ag/Alq<sub>3</sub> interface and decays along the direction perpendicular to it at the wavelength of 532 nm. We can conclude from this field distribution that the emission peak at 532 nm originates from SPP modes, as SPPs are surface waves and propagate along the interface between a metal and dielectric.

In conclusion, an enhanced efficiency OLED with corrugated nanostructures on a small-molecule organic film has been demonstrated by patterning the hole transport layer via soft nano-imprinting lithography. 24% and 20% enhancements in the luminance and current efficiency, respectively, compared with those of conventional planar devices were obtained. The observable improvement in luminance and current efficiency can be ascribed to the surface plasmonic and scattering effects caused by the Ag nanostructures. Moreover, theoretical simulations also demonstrate that the power loss to SPP modes has been recovered. This technology may provide a promising large-scale strategy for improving the efficiency of OLEDs.

The authors gratefully acknowledge the financial support from the National Natural Science Foundation of China (NSFC), the National Basic Research Program of China (973 Program), and the China Postdoctoral Science

Foundation under Grant Nos. 61322402, 61590930, 61505065, 2013CBA01700, and 2015M580246.

- <sup>1</sup>S. Reineke, F. Lindner, G. Schwartz, N. Seidler, K. Walzer, B. Lussem, and K. Leo, *Nature* **459**, 234–238 (2009).
- <sup>2</sup>B. J. Matterson, J. M. Lupton, A. F. Safonov, M. G. Salt, W. L. Barnes, and I. D. W. Samuel, *Adv. Mater.* **13**, 123–127 (2001).
- <sup>3</sup>C. F. Madigan, M.-H. Lu, and J. C. Sturm, *Appl. Phys. Lett.* **76**, 1650–1652 (2000).
- <sup>4</sup>W. H. Koo, S. M. Jeong, F. Araoka, K. Ishikawa, S. Nishimura, T. Toyooka, and H. Takezoe, *Nat. Photonics* **4**, 222–226 (2010).
- <sup>5</sup>T. Yamasaki, K. Sumioka, and T. Tsutsui, *Appl. Phys. Lett.* **76**, 1243–1245 (2000).
- <sup>6</sup>C. L. Mulder, K. Celebi, K. M. Milaninia, and M. A. Baldo, *Appl. Phys. Lett.* **90**, 211109 (2007).
- <sup>7</sup>J. M. Ziebarth, A. K. Saafir, S. Fan, and M. D. McGehee, *Adv. Funct. Mater.* **14**, 451–456 (2004).
- <sup>8</sup>S. M. Jeong, F. Araoka, Y. Machida, K. Ishikawa, H. Takezoe, S. Nishimura, and G. Suzuki, *Appl. Phys. Lett.* **92**, 083307 (2008).
- <sup>9</sup>J. R. Lawrence, P. Andrew, W. L. Barnes, M. Buck, G. A. Turnbull, and I. D. W. Samuel, *Appl. Phys. Lett.* **81**, 1955–1957 (2002).
- <sup>10</sup>Y.-G. Bi, J. Feng, Y.-F. Li, X.-L. Zhang, Y.-F. Liu, Y. Jin, and H.-B. Sun, *Adv. Mater.* **25**, 6969–6974 (2013).
- <sup>11</sup>Y. Jin, J. Feng, X.-L. Zhang, Y.-G. Bi, Y. Bai, L. Chen, T. Lan, Y.-F. Liu, Q.-D. Chen, and H.-B. Sun, *Adv. Mater.* **24**, 1187–1191 (2012).
- <sup>12</sup>Y.-G. Bi, J. Feng, Y.-F. Li, Y. Jin, Y.-F. Liu, Q.-D. Chen, and H.-B. Sun, *Appl. Phys. Lett.* **100**, 053304 (2012).
- <sup>13</sup>Y. Bai, J. Feng, Y.-F. Liu, J.-F. Song, J. Simonen, Y. Jin, Q.-D. Chen, J. Zi, and H.-B. Sun, *Org. Electron.* **12**, 1927–1935 (2011).
- <sup>14</sup>J. H. Choi, H. J. Choi, J. H. Shin, H. P. Kim, J. Jang, and H. Lee, *Org. Electron.* **14**, 3180–3185 (2013).
- <sup>15</sup>M. Cavallini, M. Murgia, and F. Biscarini, *Nano Lett.* **1**, 193–195 (2001).
- <sup>16</sup>J. You, X. Li, F.-X. Xie, W. E. I. Sha, J. H. W. Kwong, G. Li, W. C. H. Choy, and Y. Yang, *Adv. Energy Mater.* **2**, 1203–1207 (2012).
- <sup>17</sup>X. Li, W. C. H. Choy, L. Huo, F. Xie, W. E. I. Sha, B. Ding, X. Guo, Y. Li, J. Hou, J. You, and Y. Yang, *Adv. Mater.* **24**, 3046–3052 (2012).
- <sup>18</sup>K. Ishihara, M. Fujita, I. Matsubara, T. Asano, S. Noda, H. Ohata, A. Hirasawa, H. Nakada, and N. Shimoji, *Appl. Phys. Lett.* **90**, 111114 (2007).
- <sup>19</sup>S.-I. Na, S.-S. Kim, S.-S. Kwon, J. Jo, J. Kim, T. Lee, and D.-Y. Kim, *Appl. Phys. Lett.* **91**, 173509 (2007).
- <sup>20</sup>J. Wang, X. Sun, L. Chen, and S. Y. Chou, *Appl. Phys. Lett.* **75**, 2767–2769 (1999).
- <sup>21</sup>T. Granlund, T. Nyberg, L. Stolz Roman, M. Svensson, and O. Inganäs, *Adv. Mater.* **12**, 269–273 (2000).